

Implications of Three Dimensional Cloud/Aerosol Measurements in the Climate Change Issues

Teruyuki Nakajima

Center for Climate System Research, University of Tokyo

4-6-1 Komaba, Meguro-ku, Tokyo 153

(teruyuki@ccsr.u-tokyo.ac.jp)

1. Introduction

There have been intensive studies on our earth's climate system with satellite remote sensing techniques, motivated by the global warming issue due to increasing greenhouse gases. The WCRP/ISCCP (the International Satellite Cloud Climatology Project) and SRB (Surface Radiation Budget) projects, among many satellite projects, have made great contributions by finding many important scientific facts to understanding of potential climate changes. Ship track phenomenon found in the ISCCP/FIRE (First ISCCP Regional Experiment) (Coakley et al., 1987) has triggered many on-going projects of studying aerosol effects on the climate. The hypothesis of cirrus thermostat effect to stabilize the SST of tropical ocean (Ramanathan and Collins, 1991) is another topic attracting scientists for understanding the role of cirrus clouds maintaining our climate. Many field experiments, such as Japanese WCRP/WENPEX, and European ICE/EUCREX, have made many findings to understand the physical features of the cloud system (Hayasaka et al., 1995; Raschke, 1994).

In spite of such findings we still have some lack of knowledge on our climate system for improving our understanding on climate change mechanism. Many evidences of cloud-aerosol interaction have been indirectly depicted by a cloud field change with some exceptional cases of large aerosol concentration in which we can detect aerosols interacting with clouds from satellites (Kaufman and Nakajima, 1993). The value of aerosol optical thickness is less than 0.05 for most cases of important region of cloud-aerosol interaction in marine environment. This is below the detection limit of NOAA operational product of aerosol optical thickness. We also don't have good statistics of ice water content, which is necessary for better simulation of cirrus effects on climate.

Many of the above mentioned problems are related with an inability of current satellite instruments to sense the detailed vertical structure of cloud and aerosol fields. In this paper, we propose a three dimensional cloud and aerosol radiation experiment using active

satellite sensors to monitor our earth's environment.

2. A 3D cloud and aerosol radiation experiment

Effectiveness of the 94 GHz Cloud Profiling Radar (CPR) has been studied by several authors (GEWEX, 1993). According to the studies, more than 90 % of cloud cover can be detected with some exceptions of very thick deep convective clouds and very thin cirrus clouds. Recently Lite experiment has shown very impressive images of aerosol and cloud lidar signal field showing Mie Lidar (Lidar) is useful to detect cloud and aerosol field. Such impressive improvement in active sensor technology will make us ambitious to imagine a coupling of the two powerful active sensors, CPR and Lidar, in the space.

Figures 1-3 show simulated received power (W/m²) of CPR and Lidar for remote sensing of particulate constituents (water clouds, ice clouds, and aerosols) in the atmosphere as a function of particle content w (cm³/cm³) and particle radius r (μm). The Lidar can cover some region which CPR cannot measure. Especially the detection of small cloud particles and aerosols will be very important to understand the strength of cloud-aerosol interaction. The detection limit of thin clouds by CPR is around -30 dB or 0.1 g/m³ for nadir looking CPR with 1 km x 5 km resolution with 400 m height. This corresponds to the cloud optical thickness of 1.5, whereas the lidar can detect the cloud layer with optical thickness less than 3. Therefore, the combination of CPR and Lidar is very reasonable for whole range cloud detection and simultaneous aerosol detection.

3. Discussion

Combining two active sensors has many merits even for other than cloud coverage detection. The detection of cloud particle size profile is promising, since the CPR and Lidar signal have the following size dependence:

$$P_{CPR} = C_{CPR} r^6 N = C_{CPR} r^3 w, \quad (1)$$

$$P_{Lidar} = C_{Lidar} r^2 N = C_{Lidar} \frac{w}{r}. \quad (2)$$

where N is the number concentration (/cm³). As shown in Figs. 1 and 2, we can detect the particle radius as a function of height if we have both data from CPR and Lidar. This is important advantage of CPR+Lidar experiment, since the particle radius depends on height in realistic cloud and aerosol layers. Reduction of particle size, observed through aerosol-cloud interaction, will also depend on the height, since the anthropogenic aerosol source is near the surface. Especially quenching drizzle mode particles radius is an important

phenomena to observe. We will see clearer signals of those processes from the CPR+Lidar experiment.

4. Conclusion

We have discussed scientific importance of an active sensing mission of aerosol and cloud constituents. A coupling of CPR and Lidar gives us useful information, such as larger coverage of cloud and aerosol detection and cloud particle size statistics.

References

- Coakley, J. A., Jr., R. L. Bernstein, and P. A. Durkee, 1987: Effect of ship-track effluents on cloud reflectivity. *Science*, **237**, 1020-1022.
- GEWEX, 1993: Report of the GEWEX workshop on the utility and feasibility of a cloud profiling radar. Pasadena, California, June 1993.
- Hayasaka, T., T. Nakajima, Y. Fujiyoshi, Y. Ishizaka, T. Takeda, and M. Tanaka, 1995: Geometrical thickness, liquid water content and radiative properties of stratocumulus clouds over the Western North Pacific. *J. Appl. Meteor.*, **34**, 460-470.
- Kaufman, Y. J., and T. Nakajima, 1993: Effect of Amazon smoke on cloud microphysics and albedo - Analysis from satellite imagery. *J. Appl. Meteor.*, **32**, 729-744.
- Ramanathan, V., and W. Collins, 1991: Thermodynamic regulation of ocean warming by cirrus clouds deduced from observations of the 1987 El Nino. *Nature*, **351**, 27-32.
- Raschke, E., 1994: Results on cirrus properties from the European Cloud and Radiation Experiment (EUCREX)., *Proc. American Meteor. Soc. meeting*, Jan. 23-28, 1994, Nashville, Tennessee, 276-276.
- Stephens, G. L., S.-C. Tsay, P. W. Stackhouse, Jr., and P. J. Flatau, 1990: The relevance of the microphysical and radiative properties of cirrus clouds to climate and climatic feedback. *J. Atmos. Sci.*, **47**, 1742-1753.
- Suzuki, T., Tanaka, M., and T. Nakajima, 1993: The microphysical feedback of cirrus cloud in climate change. *J. Meteor. Soc. Japan*, **71**, 701-713.

Water clouds with the top at 4km

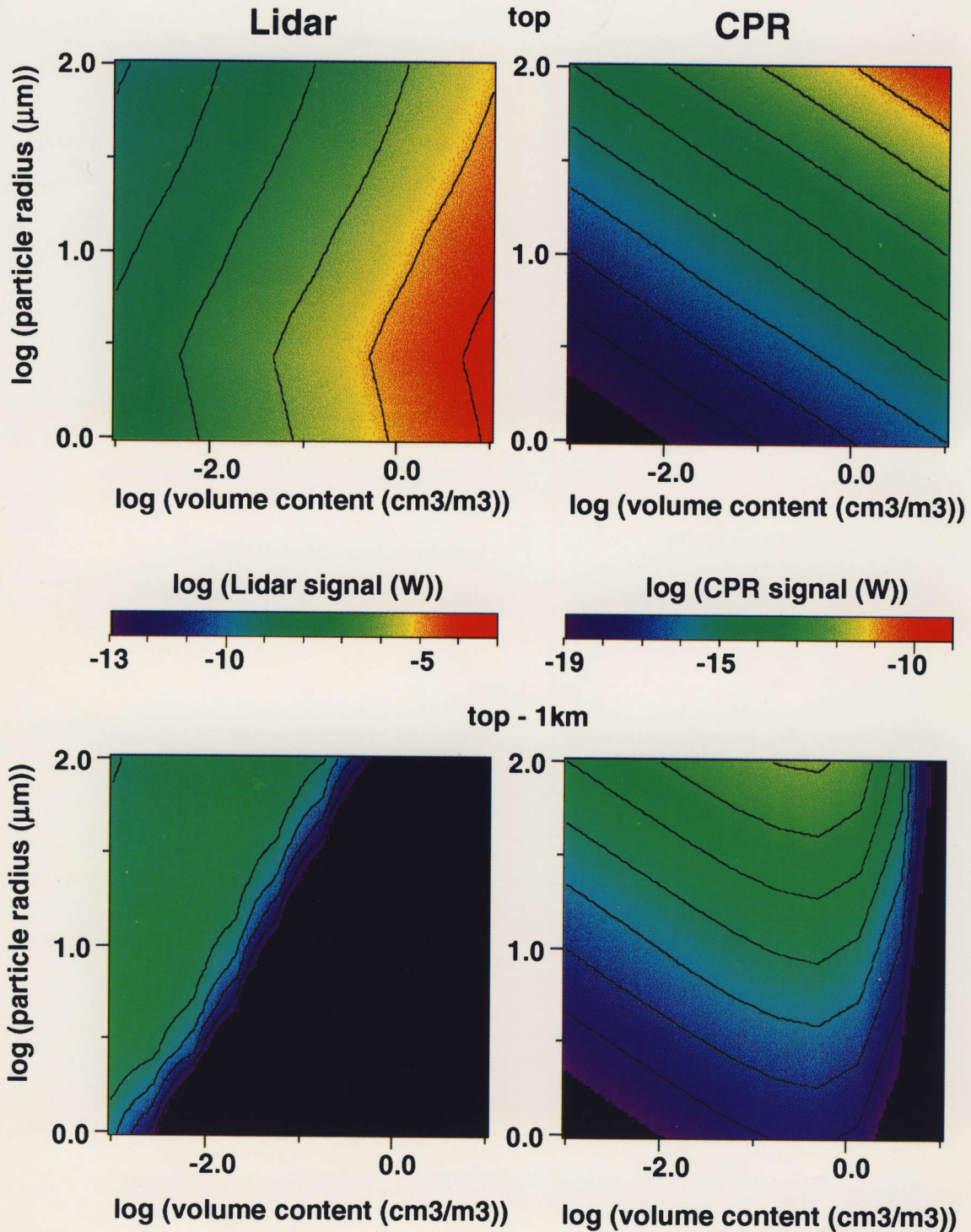


Fig. 1 CPR and Lidar signals for water clouds with 1 km thickness and layer top height of 4 km. as a function of volume content (cm^3/cm^3) and particle radius (μm) Upper and lower panels show signals from layer top and bottom, respectively.

Ice clouds with the top at 10km

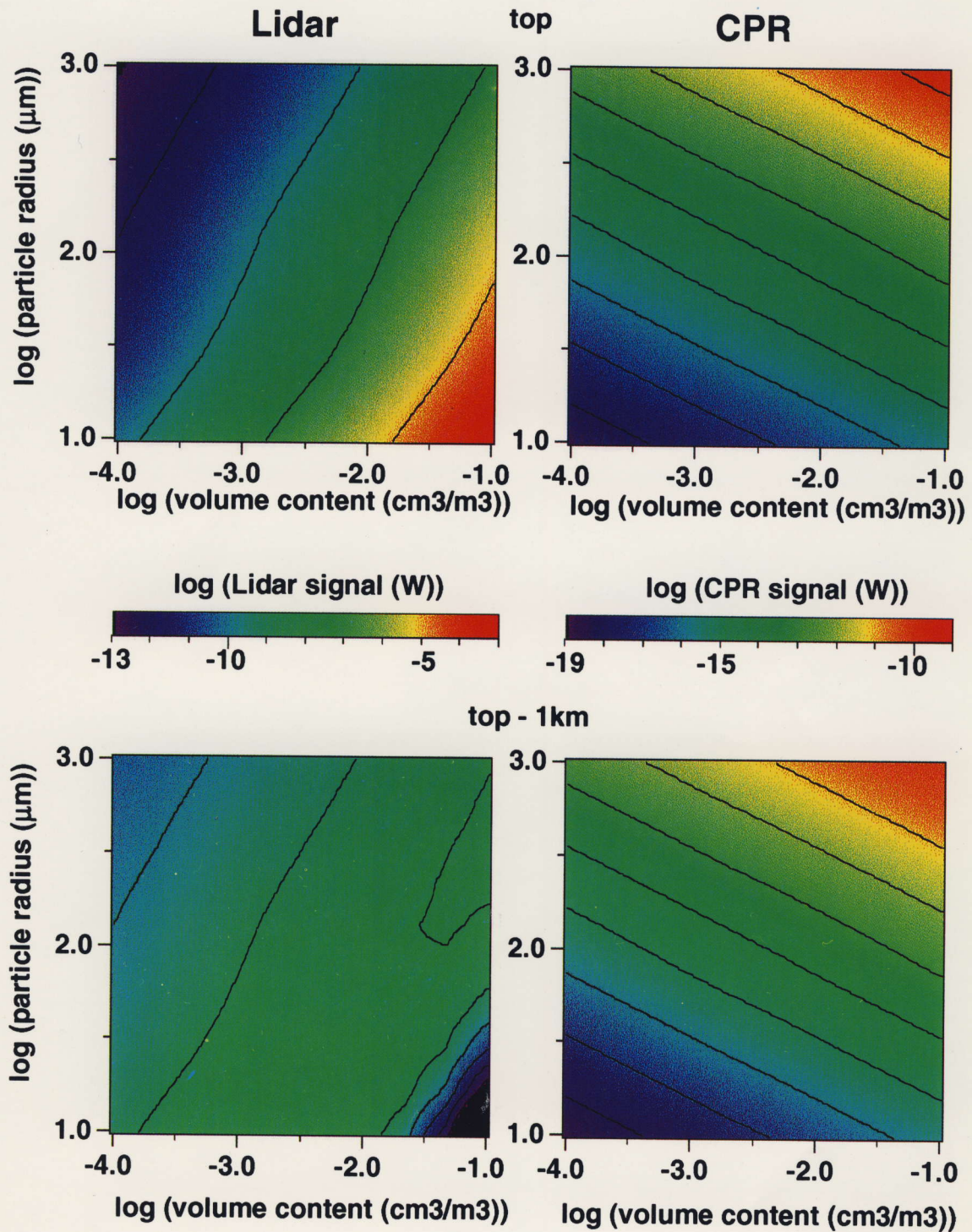


Fig. 2 Same as Fig. 1 but for ice clouds with 1 km thickness and layer top height of 10 km.

Aerosol layers with the top at 1km

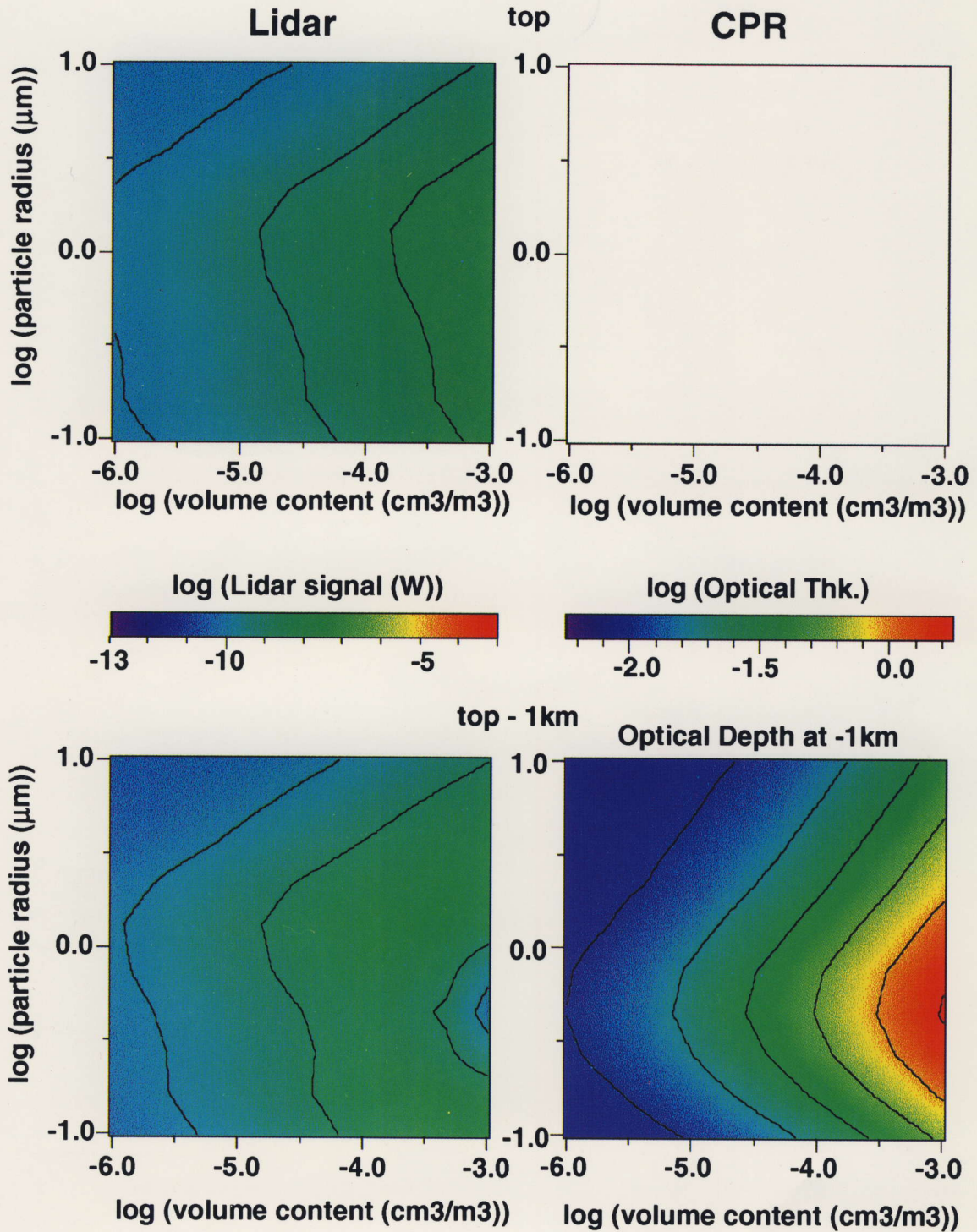


Fig. 3 Same as Fig. 1 but for aerosols with 1 km thickness and layer top height of 1 km.

Implications of Three Dimensional Cloud/Aerosol Measurement in the Climate Change Issues

Teruyuki Nakajima

Center for Climate System Research, University
4-6-1 Komaba, Meguro-ku, Tokyo 153
(teruyuki@ccsr.u-tokyo.ac.jp)

- ☆ Global warming issues
- ☆ CPR + Lidar experiment (ATMOS-B1 mission)

Global warming issues for the CPR + Lidar experiment

1. Aerosol direct forcing

$$\Delta\tau_{SO_4} = 0.04, \quad \Delta F = -1.3 \text{ W/m}^2 \quad (\text{Charlson et al., 1992})$$

2. Aerosol-cloud interaction

$$N/N_0 = 1.15, \quad \Delta F = -1.0 \text{ W/m}^2 \quad (\text{Charlson et al., 1992})$$
$$-0.3 \text{ W/m}^2 \sim -1.5 \text{ W/m}^2$$

3. Cloud top/base height

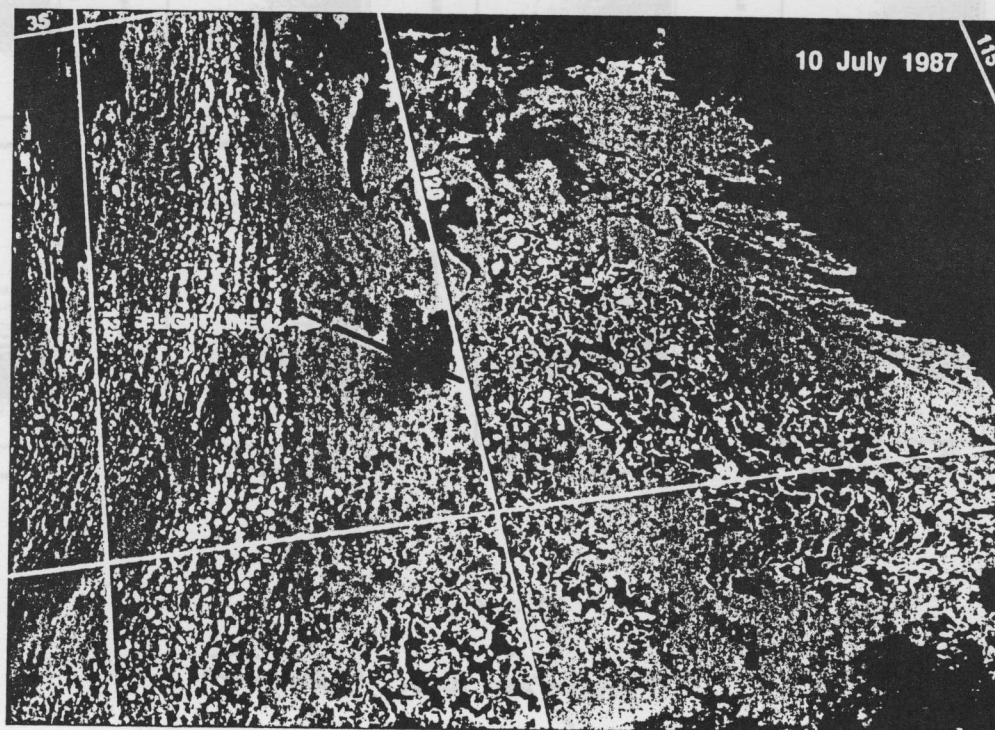
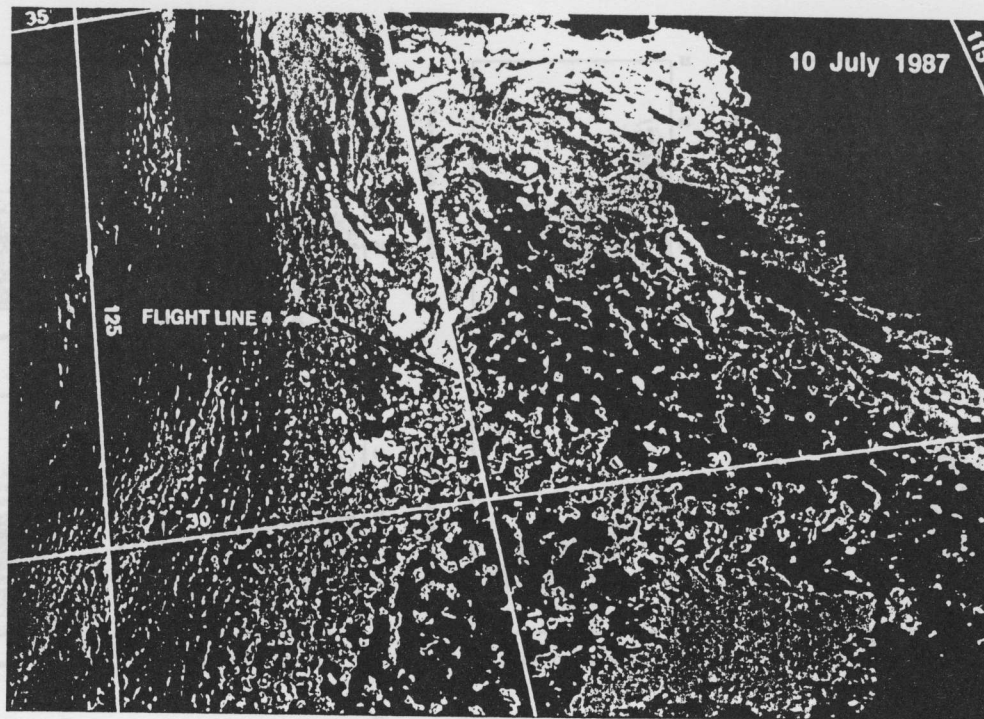
$$\Delta T_{top} \uparrow\downarrow?, \quad \Delta T_{base} \uparrow\downarrow?$$

4. Upper cloud amount/phase

$$n \uparrow\downarrow?, \quad w_{ice} \uparrow\downarrow?$$

* Those issues will need statistics first.

Climate effects of cirrus clouds



カリフォルニア沖における夏期層積雲の微物理構造のリモートセンシング。光学的厚さ（上）と雲粒の等価半径（下）をAVHRRから求めたもの。1987年7月10日の例。図の左側には海洋気団の影響を受けた薄く霧粒を伴った雲、右側には大陸性気団の影響を受けた厚く粒径が小さな雲が存在することが分かる。

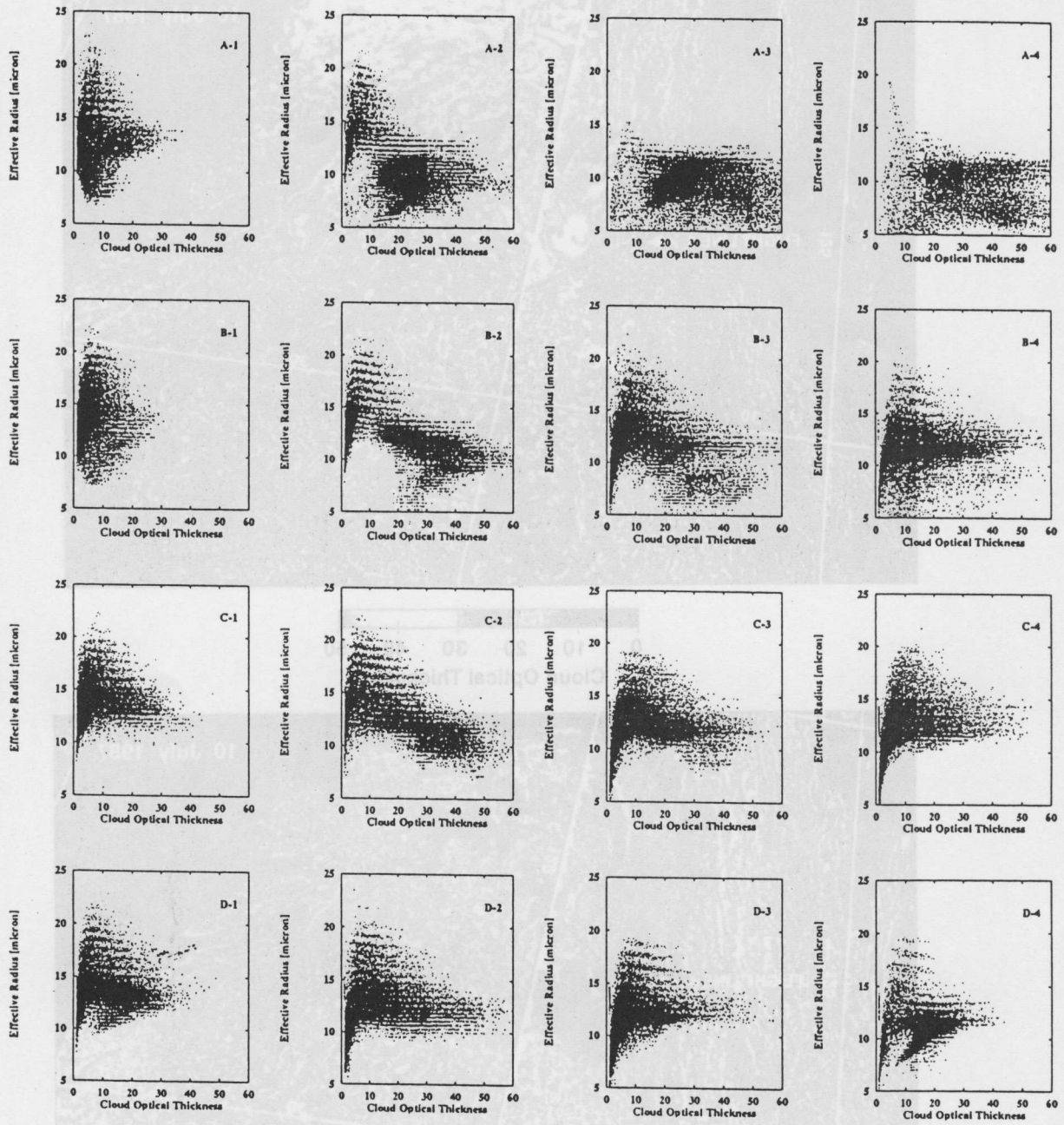


Fig. 17
 Nakajima and Nakajima

Effective Radius

光。くぐくぐサイーチーの道の機物理量の雲層間夏るはに中てニホアてリてハ
 月7年7801。のよため来さやRPHVAき(下)登半面等の雲う(上)ち観の学
 以観は、雲とを付き登霧>観たか受き登雲の図。時の日01
 。るは分たるこるすき登が雲なち小が登霧>観たか受き登雲の図。時の日01

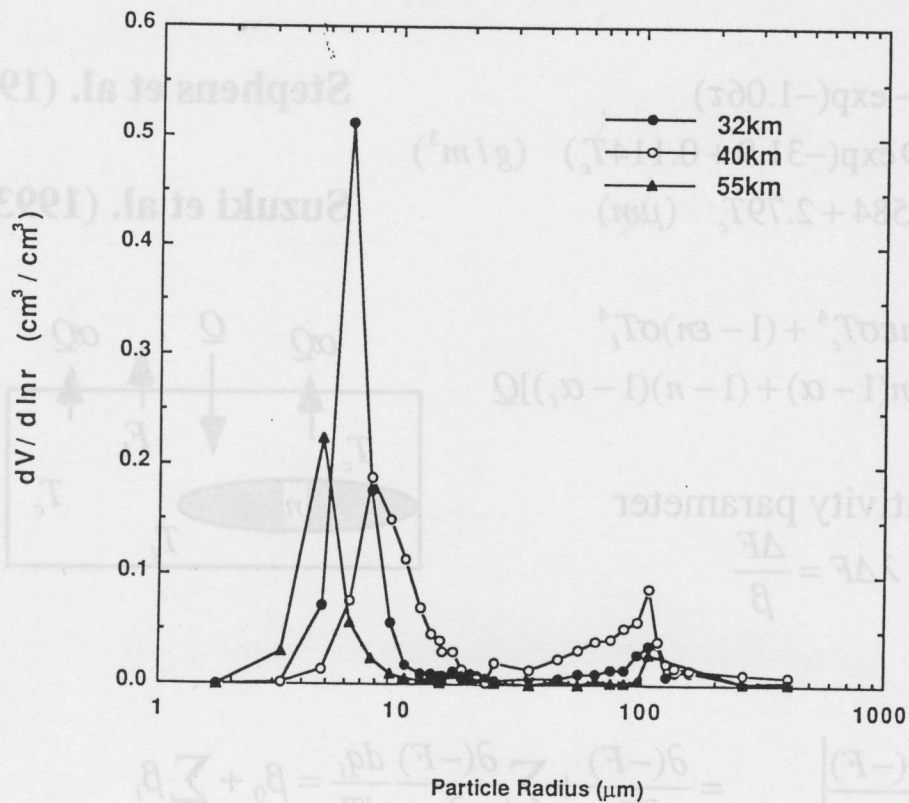
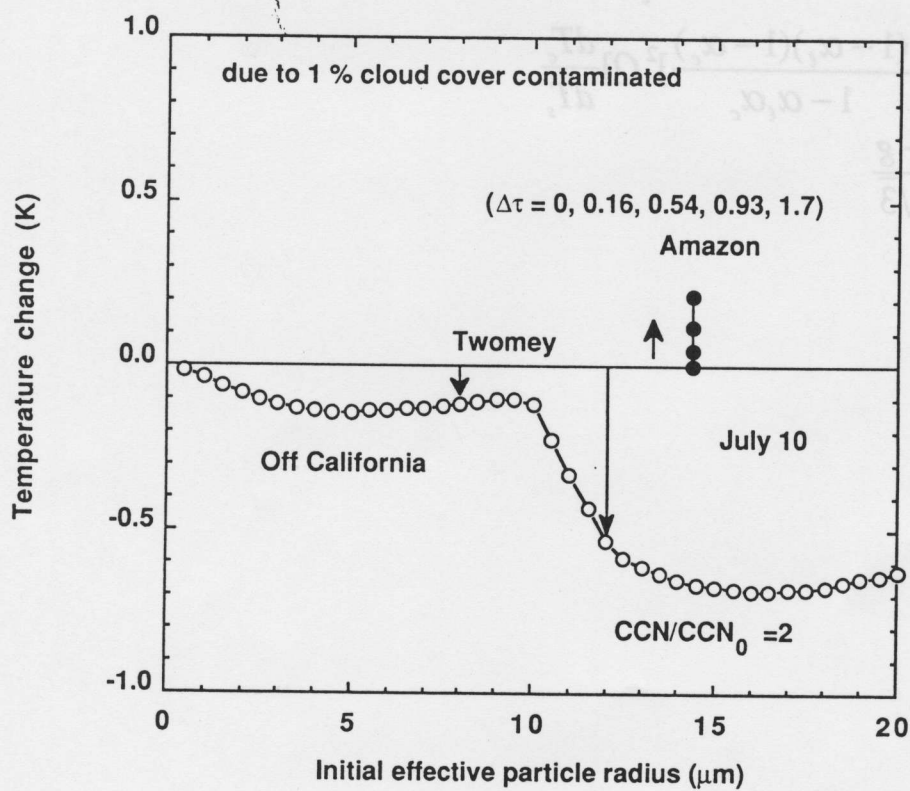


Fig. 3 Volume spectra of cloud particle polydispersion at flight distance of 32, 40 and 55 km along the center of the images shown in Fig. 2.



$$\varepsilon = 1 - \exp(-1.06\tau)$$

$$w = D \exp(-31.9 + 0.114T_c) \quad (\text{g/m}^3)$$

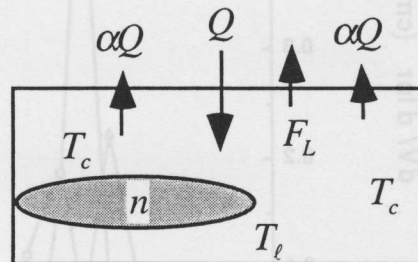
$$r_e = -584 + 2.79T_c \quad (\mu\text{m})$$

Stephens et al. (1990)

Suzuki et al. (1993)

$$F_L = n\varepsilon\sigma T_c^4 + (1 - \varepsilon n)\sigma T_\ell^4$$

$$F_S = [n(1 - \alpha) + (1 - n)(1 - \alpha_\ell)]Q$$



Sensitivity parameter

$$\Delta T_s = \lambda \Delta F = \frac{\Delta F}{\beta}$$

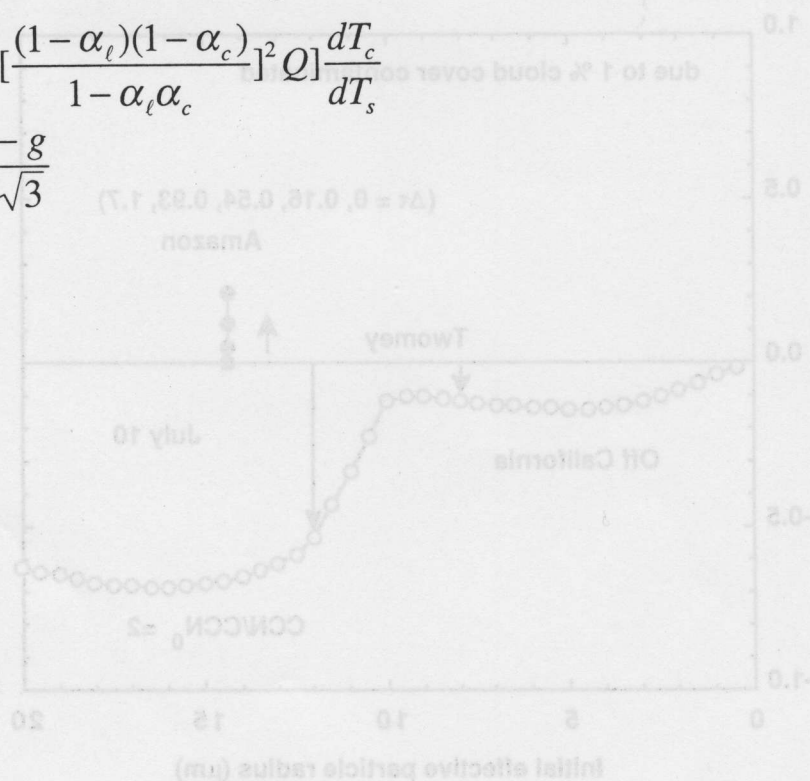
$$\beta = \left. \frac{d(-F)}{dT_s} \right|_{e \rightarrow e+de} = \frac{\partial(-F)}{\partial T_s} + \sum_i \frac{\partial(-F)}{\partial q_i} \frac{dq_i}{dT_s} = \beta_0 + \sum_i \beta_i$$

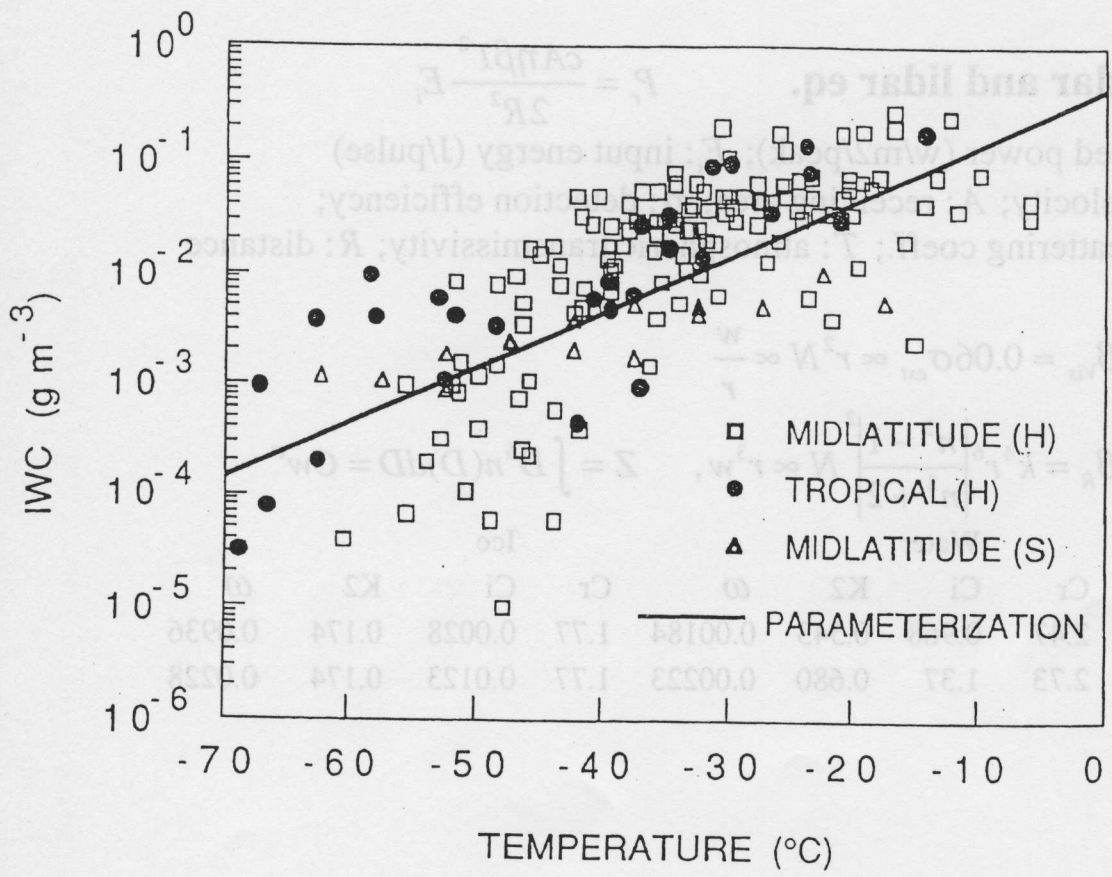
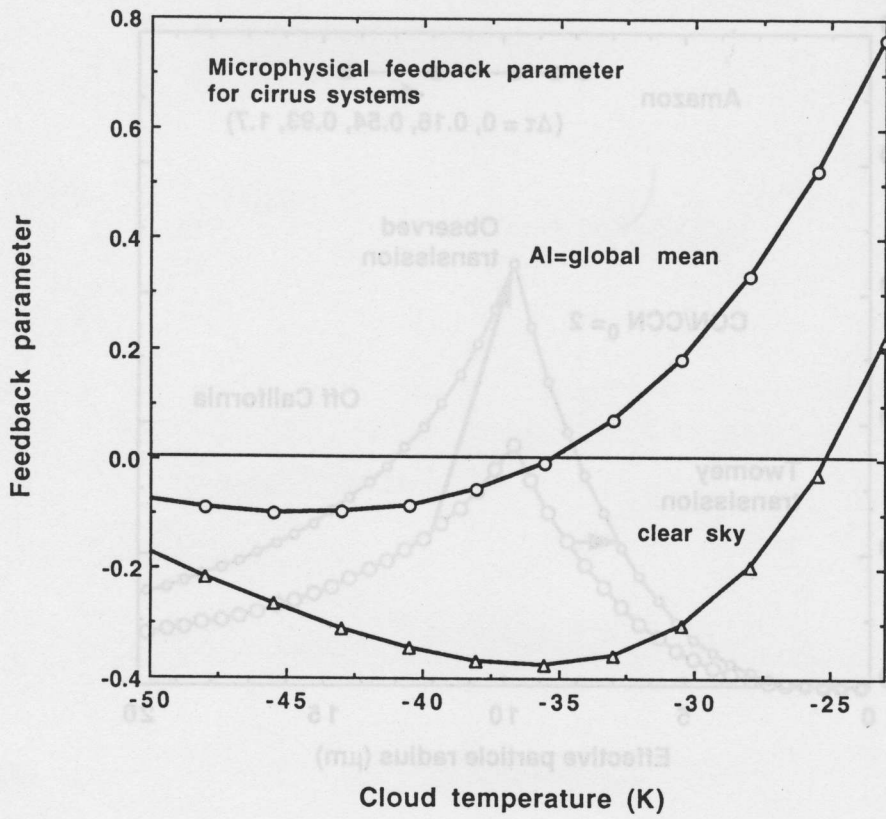
$$\beta_n = [\varepsilon\sigma(T_c^4 - T_\ell^4) + (\alpha - \alpha_\ell)Q] \frac{dn}{dT_s}$$

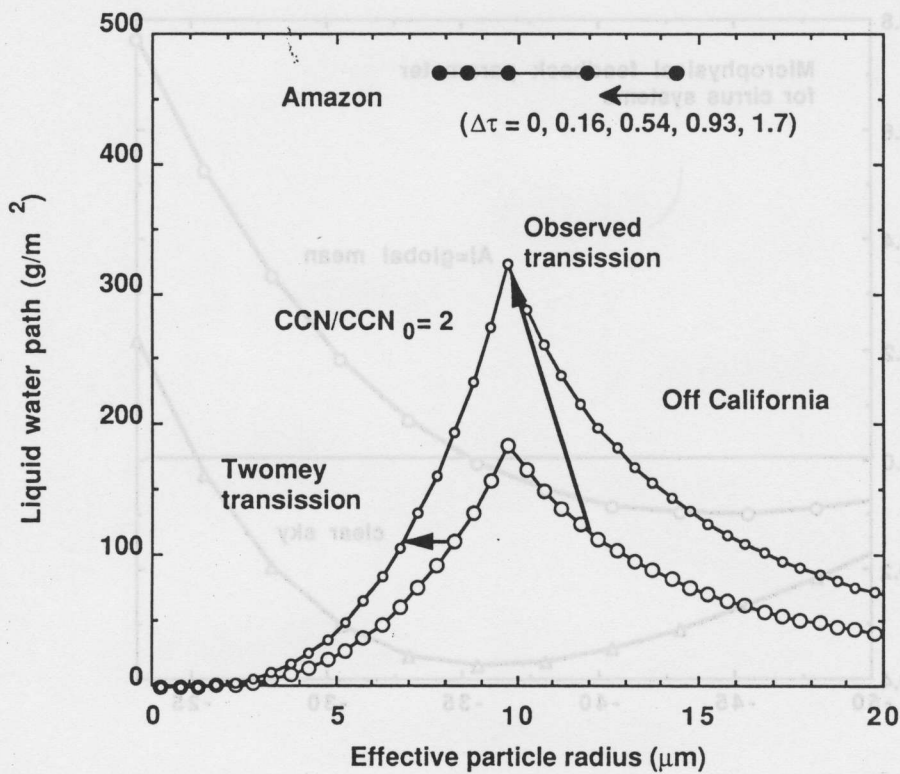
$$\beta_{micro} = 0.114n\tau_c \left(1 - \frac{24.5}{r_e}\right) \{1.06(1 - \varepsilon)\sigma(T_c^4 - T_\ell^4)$$

$$+ \eta \left[\frac{(1 - \alpha_\ell)(1 - \alpha_c)}{1 - \alpha_\ell \alpha_c} \right]^2 Q \} \frac{dT_c}{dT_s}$$

$$\eta = \frac{1 - g}{2\sqrt{3}}$$







Radar and lidar eq.

$$P_r = \frac{cA\eta\beta T^2}{2R^2} E_i$$

P_r : received power (w/m²/peak); E_i : input energy (J/pulse)
 c : light velocity; A : receiving area; η : detection efficiency;
 β : backscattering coeff.; T : atmospheric transmissivity; R : distance

$$\beta_{Vis} \approx 0.06\sigma_{ext} \propto r^2 N \propto \frac{w}{r}$$

$$\beta_R = k^4 r^6 \left| \frac{n^2 - 1}{n^2 + 2} \right|^2 N \propto r^3 w, \quad Z = \int D^6 n(D) dD = Cw^\alpha$$

Temp	Water				Ice			
	Cr	Ci	K2	ω	Cr	Ci	K2	ω
259.0	2.47	0.968	0.543	0.00184	1.77	0.0028	0.174	0.0936
272.0	2.73	1.37	0.680	0.00223	1.77	0.0123	0.174	0.0228

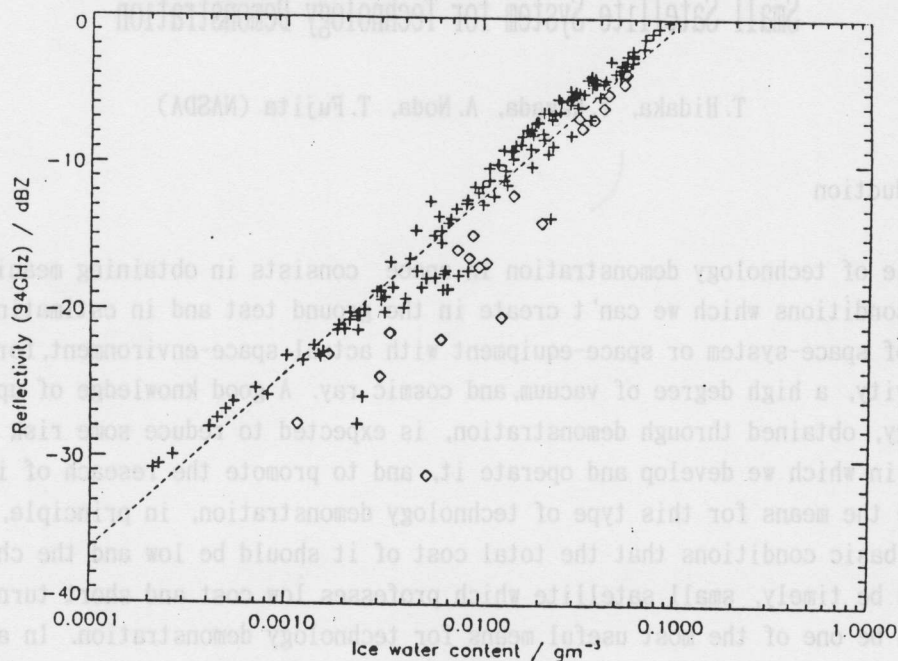


Figure 4. Values of ice water content (IWC) and reflectivity computed from cirrus ice particle size spectra observed by the Meteorological Office C-130 aircraft. [+ data for two vertical profiles; ◊ data for level runs on different days]

w-r statistics of clouds

